Annals of Nuclear Energy 99 (2017) 68–79

Contents lists available at ScienceDirect

Annals of Nuclear Energy

journal homepage: www.elsevier.com/locate/anucene

Spectral properties of dynamic processes in a nuclear reactor

Alexander V. Avvakumov [a], Valery F. Strizhov [b], Petr N. Vabishchevich [b,c,*], Alexander O. Vasilev [c]

[a] National Research Center Kurchatov Institute, 1, Sq. Academician Kurchatov, Moscow, Russia
[b] Nuclear Safety Institute, Russian Academy of Sciences, 52, B. Tulskaya, Moscow, Russia
[c] North-Eastern Federal University, 58, Belinskogo, Yakutsk, Russia

ARTICLE INFO

Article history:
Received 6 April 2016
Received in revised form 24 July 2016
Accepted 12 September 2016

Keywords:
Neutron diffusion equation
Multi-group approximation
Space-time kinetic
Spectral problem
Regular regime of time-dependent process

ABSTRACT

As a rule, mathematical modeling of dynamic processes in nuclear reactors is conducted using an approach that treats a neutron flux in the multigroup diffusion approximation. In this approach, the basic model involves a multidimensional system of coupled parabolic-type equations. Similarly to common thermal phenomena, it is possible here to separate a regular mode of nuclear reactor operation that is associated with a selfsimilar development of a neutron field at large times. In this case, the main feature of dynamic processes is a minimal eigenvalue of the corresponding spectral problem. In the present paper, calculations of various eigenvalues are performed via the two-group model and discussed for the VVER-1000 reactor without a reflector and HWR reactor.

1. Introduction

The physical processes in a nuclear reactor (Duderstadt and Hamilton, 1976) depend on distribution of neutron flux, whose mathematical description is based on the neutron-transport equation (Hetrick, 1971; Stacey, 2007). The general view of this equation is integro-differential one, and the required distribution of neutrons flux depends on time, energy, spatial and angular variables. As a rule, the simplified forms of the neutron transport equation are used for practical calculations of nuclear reactors. The equation system that is known as a multigroup diffusion approach is mostly used for reactor analysis (Marchuk and Lebedev, 1986; Lewis and Miller, 1993; Sutton and Aviles, 1996; Cho, 2005) and is applied in most engineering calculation codes.

Modern reactor simulations are actually based on transport calculations (see, for example, Smith and Rhodes, 2002; Sanchez, 2012; Boyd et al., 2014). In multiscale reactor-physics simulations diffusion models are derived and applied using sophisticated homogenization methodologies Sanchez (2009) which define parameters of the multigroup diffusion equations that enable one to take into account transport effects. The homogenization methodologies use solution of specially defined transport problems to generate homogenized cross sections for the multigroup diffusion equations. Most of current methodologies (see, for example, Sanchez (2009)) use k-eigenvalue transport problems to calculate averaging shape functions. Recently Dugan et al. (2016) developed advanced homogenization methods apply α-eigenvalue transport problems.

The standard methods of approximate solutions of non-stationary problems are used for modelling of the dynamics of neutron-physical processes. The most attention is paid to two-level schemes with weights (θ-method) (Ascher, 2008; LeVeque, 2007; Hundsdorfer and Verwer, 2003), the Runge–Kutta and Rosenbrock schemes (Butcher, 2008; Hairer and Wanner, 2010) are used. Let's note a special class of methods for modelling of non-stationary neutron transport in diffusion multigroup approximation, which is connected with multiplicative representation of solution — space–time factorization methods and the quasistatic method (Chou et al., 1990; Dahmani et al., 2001; Dodds, 1976; Goluoglu and Dodds, 2001). The approximate solution is searched in the form of the product of two functions, one of which depends on time and is related to the amplitude, the second one (the shape function) describes the spatial distribution. It is difficult to check the accuracy of the approximate solution in such approach, in particular, while calculating the dynamic modes with complicated changes in neutron flux distribution.

The processes occurring in a nuclear reactor are essentially non-stationary. The stationary state of neutron flux, which is related to the critical state of the reactor, is characterised by local balancing of neutron absorption and generation. This boundary state is usually described by solution of a spectral problem (Lambda Modes

* Corresponding author at: Nuclear Safety Institute, Russian Academy of Sciences, 52, B. Tulskaya, Moscow, Russia.
E-mail addresses: Avvakumov2009@rambler.ru (A.V. Avvakumov), vfs@ibrae.ac.ru (V.F. Strizhov), vabishchevich@gmail.com (P.N. Vabishchevich), haska87@gmail.com (A.O. Vasilev).

http://dx.doi.org/10.1016/j.anucene.2016.09.021
0306-4549/

problem, λ-eigenvalue problem) provided that the fundamental eigenvalue (maximal eigenvalue) that is called k-effective of the reactor core, is equal to unity. In this case, the stationary neutron field is related with the corresponding eigenfunction. Calculations of k-effective of the reactor on the basis of the spectral Lambda Modes problem solution are obligatory for developing a new design of reactor installation.

Time behaviour of nuclear reactor is deemed sometimes to be related to the deviation of k-effective from unity that involves, in particular, concept of reactivity. This is not justified, since, while calculating this parameter, the evolutionary nature of neutron redistribution processes (nonstationary systems of the equations) is considered in no way. The k-effective parameter deviates from unity, though quite weakly, but anyway such a solution, generally speaking, cannot be connected with the stationary solution of the problem. There is simply no such a solution. Thus, the attempts to correct the basic mathematical model of non-stationary neutron diffusion by introducing some correcting multipliers to achieve the strict criticality are not successful.

The spectral parameter α, which is not directly connected with k-effective, is proposed to be used instead of k-effective for more adequate characteristic of the dynamic nature of reactor. It is defined as the fundamental eigenvalue of the spectral problem (time-eigenvalue, α-eigenvalue problem), which is connected with the non-stationary equations of neutron diffusion (Bell and Glasstone, 1970; Modak and Gupta, 2007; Verdu et al., 2010). By analogy with the usual problems of heat conductivity (see, for example, Luikov, 1968; Samarskii and Vabishchevich, 1996) we consider the regular reactor mode. At large times the behavior of a neutron flux is asymptotic, and one can talk about space–time factorization solution, whose amplitude is $\exp(\alpha t)$, the shape function is the eigenfunction of the spectral problem.

The Lambda and Alpha Modes spectral problems deal with a not self-adjoint vector elliptic operator. Generally, the eigenvalues are complex. The strict conclusion concerning the eigenvalue reality was obtained (see, for instance, Habetler and Martino, 1961) under reasonable physics assumptions only for the fundamental eigenvalue. Performed precise calculations of the reactor test problems (the VVER-1000 reactor without a reflector and HWR reactor) confirm the fact that the next eigenvalues may be complex with small imaginary parts. Our investigation clarifies the results of other authors (González-Pintor et al., 2009), which give only real parts of the eigenvalue for the same test problems. These clarifications deal with the accuracy control during eigenvalue and eigenfunction calculations using a set of fine meshes and finite elements of different degree; also we used applied software aimed to solve spectral problems with not self-adjoint operators.

Study of the dynamic processes can be based on the discrimination of symmetric and skew-symmetrical parts of the neutron transport operator. In this case, we can easily get the a priori assessments of stability in the corresponding norm, while assessing the operator of the symmetric part from below, and perform the analysis of used time approximations (Samarskii, 2001; Samarskii et al., 2002). To get this, the partial spectral problem is solved to find the fundamental eigenvalue δ of the Delta Modes spectral problem.

The paper is organised as follows. The statement of the boundary-value problem for the system of non-stationary diffusion equations in multigroup approach is given in Section 2. Various spectral problems are discussed in Section 3. A numerical example of calculation of spectral characteristics within the frameworks of two-dimensional test problems for VVER-1000 reactor and HWR reactor using the two-group system of diffusion equations is discussed in Section 4. The results of the work are summarised in Section 5.

2. Problem statement

The neutron flux is considered in multigroup diffusion approximation. The neutron dynamics is considered in the limited convex two-dimensional or three-dimensional area $\Omega(\boldsymbol{x} = \{x_1, \ldots, x_d\} \in \Omega,\ d = 2, 3)$ with boundary $\partial\Omega$. The neutron transport is described by the system of equations:

$$\frac{1}{v_g}\frac{\partial \phi_g}{\partial t} - \nabla \cdot D_g \nabla \phi_g + \Sigma_{rg}\phi_g - \sum_{g \neq g'=1}^{G} \Sigma_{s,g' \to g}\phi_{g'} = (1-\beta)\chi_g \sum_{g'=1}^{G} \nu\Sigma_{fg'}\phi_{g'} + \widetilde{\chi}_g \sum_{m=1}^{M} \lambda_m c_m, \quad g = 1, 2, \ldots, G. \tag{1}$$

Here $\phi_g(\boldsymbol{x}, t)$ — neutron flux of g group at point $\boldsymbol{x}$ and time t, G — number of energy groups, v_g — effective velocity of neutrons in the group g, $D_g(\boldsymbol{x})$ — diffusion coefficient, $\Sigma_{rg}(\boldsymbol{x}, t)$ — removal cross-section, $\Sigma_{s,g' \to g}(\boldsymbol{x}, t)$ — scattering cross-section from group g' to group g, β — effective fraction of delayed neutrons, $\chi_g, \widetilde{\chi}_g$ — spectra of prompt and delayed neutrons, $\nu\Sigma_{fg}(\boldsymbol{x}, t)$ — generation cross-section of group g, c_m — density of sources of delayed neutrons of m-type, λ_m — decay constant of sources of delayed neutrons, M — number of types of delayed neutrons. The density of sources of delayed neutrons is described by the equations:

$$\frac{\partial c_m}{\partial t} + \lambda_m c_m = \beta_m \sum_{g=1}^{G} \nu\Sigma_{fg}\phi_g, \quad m = 1, 2, \ldots, M, \tag{2}$$

where β_m is a fraction of delayed neutrons of m-type, and

$$\beta = \sum_{m=1}^{M} \beta_m.$$

System of Eqs. (1) and (2) is supplemented with corresponding initial and boundary conditions.

The albedo-type conditions are set at the boundary $\partial\Omega$ of the area Ω:

$$D_g \frac{\partial \phi_g}{\partial n} + \gamma_g \phi_g = 0, \qquad g = 1, 2, \ldots, G, \tag{3}$$

where n — outer normal to the boundary $\partial\Omega$.

Let's propose that the reactor was critical up to the initial time moment ($t = 0$):

$$\phi_g(x, 0) = \phi_g^0(x), \quad c_m(x, 0) = c_m^0(x). \tag{4}$$

For $\phi_g^0(x)$ and $c_m^0(x)$ we get:

$$-\nabla \cdot D_g \nabla \phi_g^0 + \Sigma_{rg}\phi_g^0 - \sum_{g \neq g'=1}^{G} \Sigma_{s,g' \to g}\phi_{g'}^0 = \left((1-\beta)\chi_g + \beta\widetilde{\chi}_g\right) \sum_{g'=1}^{G} \nu\Sigma_{fg'}\phi_{g'}^0, \quad g = 1, 2, \ldots, G,$$

$$\lambda_m c_m^0 = \beta_m \sum_{g=1}^{G} \nu\Sigma_{fg}\phi_g^0, \quad m = 1, 2, \ldots, M.$$

Let's consider the problem without taking into account delayed neutrons (all neutrons are prompt). We assume that all neutrons (including delayed neutrons) are born as prompt, but their spectra χ_g and $\widetilde{\chi}_g$ are different. Then instead of (1) one can obtain the following equation:

$$\frac{1}{v_g}\frac{\partial \phi_g}{\partial t} - \nabla \cdot D_g \nabla \phi_g + \Sigma_{rg}\phi_g - \sum_{g \neq g'=1}^{G} \Sigma_{s,g' \to g}\phi_{g'} = \left((1-\beta)\chi_g + \beta\widetilde{\chi}_g\right) \sum_{g'=1}^{G} \nu\Sigma_{fg'}\phi_{g'}, \quad g = 1, 2, \ldots, G. \tag{5}$$

The problem for Eq. (5) is solved with boundary conditions of form (3) and the following initial conditions:

$$\phi_g(x,0) = \phi_g^0(x), \quad g = 1,2,\ldots,G. \tag{6}$$

Let's write the boundary problem (3), (5), (6) in operator form. The vector $\phi = \{\phi_1, \phi_2, \ldots, \phi_G\}$ and matrices are defined as follows:

$$V = (v_{gg'}), \quad v_{gg'} = \delta_{gg'} v_g^{-1},$$

$$D = (d_{gg'}), \quad d_{gg'} = -\delta_{gg'} \nabla \cdot D_g \nabla,$$

$$S = (s_{gg'}), \quad s_{gg'} = \delta_{gg'} \Sigma_{rg} - \Sigma_{s,g'\to g},$$

$$R = (r_{gg'}), \quad r_{gg'} = ((1-\beta)\chi_g + \beta\widetilde{\chi}_g)\nu\Sigma_{fg'},$$

$$L = (l_{gg'}), \quad l_{gg'} = \delta_{gg'}\gamma_g,$$

$$g, g' = 1,2,\ldots,G,$$

where

$$\delta_{gg'} = \begin{cases} 1, & g = g', \\ 0, & g \neq g', \end{cases}$$

is the Kronecker symbol. We shall use the set of vectors ϕ, whose components satisfy the boundary conditions (3). Using the set definitions, the system of Eqs. (5) can be written in the form of first-order equation of evolution:

$$V\frac{d\phi}{dt} + (D+S)\phi = R\phi. \tag{7}$$

The Cauchy problem is solved for (7), when

$$D\frac{d\phi}{dn} + L\phi = 0, \quad \phi(0) = \phi^0, \tag{8}$$

where (see (6)) $\phi^0 = \{\phi_1^0, \phi_2^0, \ldots, \phi_G^0\}$.

3. Spectral problems

To characterize the reactor dynamic processes described by Cauchy problem (7) and (8), let's consider some spectral problems Bell (Bell and Glasstone, 1970; Hetrick, 1971; Stacey, 2007).

The following spectral problem is usually solved:

$$(D+S)\varphi = \lambda^{(k)} R\varphi. \tag{9}$$

This problem (9) is known as the Lambda Modes problem for a given configuration of the reactor core. The minimal eigenvalue is used for characterisation of neutron field, thus

$$k = \frac{1}{\lambda_1^{(k)}}$$

is the effective multiplication factor (k-effective). The value $k = 1/\lambda_1^{(k)} = 1$ is related to the critical state of the reactor, and the corresponding eigenfunction $\varphi_1(x)$ is the stationary solution of the Eq. (7). At $k > 1$, one can speak about supercriticality, at $k < 1$ — about subcriticality.

Due to nonself-adjoint operators of neutron transport we have, generally speaking, the complex eigenvalues. The reality and positivity property of the fundamental eigenvalue for the system of neutronics equations is proved using the principle of maximum at some restrictions on factors of neutron transport operators (Habetler and Martino, 1961). This is also true for the nonself-adjoint elliptic operator of the second order (Evans, 1998).

The spectral problem (9) cannot directly be connected with the dynamic processes in a nuclear reactor. At the best, we can get only the limiting case — the stationary critical state. The more acceptable spectral characteristics for the non-stationary Eq. (7) are related the spectral problem

$$A\varphi = \lambda^{(\alpha)} V\varphi, \quad A = D + S - R. \tag{10}$$

The fundamental eigenvalue

$$\alpha = \lambda_1^{(\alpha)}$$

is called Bell and Glasstone (1970) α–eigenvalues or period eigenvalues, because they are inversely related to the reactor periods. The asymptotic behaviour of Cauchy problem solution (7) and (8) at large times can be connected with the eigenvalue α. In this regular mode, the reactor behaviour is described by the function $\exp(-\alpha t)\varphi_1(x)$. Critical state of the reactor is defined at $\alpha = 0$; when $\alpha > 0$ we get the supercritical state, and when $\alpha < 0$ — subcritical state of the reactor.

A priori assessments of solution at the current time are used to characterize the evolution processes (Evans, 1998). Let's define the Hilbert space $H = L_2(\Omega)$, for vector functions, in which the scalar product $(\cdot,\cdot)$ and norm $\|\cdot\|$ are as follows:

$$(\phi,\varphi) = \sum_{g=1}^{G}(\phi_g,\varphi_g), \quad \|\phi\| = (\phi,\phi)^{1/2},$$

where

$$(\phi_g,\varphi_g) = \int_\Omega \phi_g(x)\varphi_g(x)\,dx, \quad g = 1,2,\ldots,G.$$

Let's select the self-adjoint and skew-symmetric parts in the operator A:

$$A = A_1 + A_2, \quad A_1 = A_1^* = \frac{1}{2}(A + A^*), \quad A_2 = -A_2^* = \frac{1}{2}(A - A^*).$$

The diffusion operator D is self-adjoint at the set of functions satisfying the boundary conditions (3): $D = D^*$. For A_1 and A_2 we get

$$A_1 = \left(a_{gg'}^{(1)}\right), \quad A_2 = \left(a_{gg'}^{(2)}\right),$$

$$a_{gg'}^{(1)} = -\delta_{gg'}\nabla\cdot D_g\nabla + \delta_{gg'}\Sigma_{rg} - \frac{1}{2}\left(\Sigma_{s,g'\to g} + \Sigma_{s,g\to g'}\right) - \frac{1}{2}\left(((1-\beta)\chi_g + \beta\widetilde{\chi}_g)\nu\Sigma_{fg'} + ((1-\beta)\chi_{g'} + \beta\widetilde{\chi}_{g'})\nu\Sigma_{fg}\right),$$

$$a_{gg'}^{(2)} = -\frac{1}{2}\left(\Sigma_{s,g'\to g} - \Sigma_{s,g\to g'}\right) - \frac{1}{2}\left(((1-\beta)\chi_g + \beta\widetilde{\chi}_g)\nu\Sigma_{fg'} - ((1-\beta)\chi_{g'} + \beta\widetilde{\chi}_{g'})\nu\Sigma_{fg}\right).$$

Let's consider the spectral problem

$$A_1\varphi = \lambda^{(\delta)} V\varphi \tag{11}$$

for the self-adjoint part of the operator A. All eigenvalues of the Delta Modes spectral problem (11) are real.

Let us find the fundamental eigenvalue in (7) and (8), to characterize the dynamic processes described by the problem (11):

$$\delta = \lambda_1^{(\delta)},$$

and (see, e.g., Hogben, 2013, Section 16.1) $\delta \leqslant \alpha$. Taking into account the skew-symmetry of A_2 we obtain

$$(A\phi,\phi) = (A_1\phi,\phi) \geqslant \delta(V\phi,\phi),$$

i.e.

$$A \geqslant \delta V. \tag{12}$$

Based upon the assessment (12) the corresponding priori assessment for the Cauchy problem solution (7) and (8) is set.

Let us connect the operator $V = V^* > 0$ with the Hilbert space H_V, in which the scalar product and norm are

$$(\phi, \varphi)_V = (V\phi, \varphi), \quad \|\phi\|_V = (\phi, \phi)_V^{1/2}.$$

Scalar multiplying in H the Eq. (7) by ϕ and taking into account (12), we obtain:

$$\left(V\frac{d\phi}{dt}, \phi\right) + \delta(V\phi, \phi) \leqslant 0.$$

Taking into account

$$\left(V\frac{d\phi}{dt}, \phi\right) = \frac{1}{2}\frac{d}{dt}(V\phi, \phi) = \|\phi\|_V \frac{d}{dt}\|\phi\|_V,$$

we get

$$\frac{d}{dt}\|\phi\|_V + \delta\|\phi\|_V \leqslant 0.$$

Considering the initial condition (8), based upon the Grönwall's lemma we come to an a priori assessment:

$$\|\phi(t)\|_V \leqslant \exp(-\delta t)\|\phi^0\|_V \tag{13}$$

for the solution of the problem (7) and (8). Such assessments expressing the stability of the solution against the initial data, are the reference points, while constructing the time approximations (Samarskii, 2001; Samarskii et al., 2002).

The spectral problem (11) is more convenient for numerical solving than the spectral problems (9) and (10) (Golub and Van Loan, 2012; Saad, 2011). This is explained by the fact that in this case, all eigenvalues and eigenfunctions are real. The value δ defines not only the criticality of the reactor (at $\delta = 0$), but also the dynamics of the neutron field of the reactor — see the assessment (13).

The k-eigenvalue of the Lambda Modes spectral problem (9), namely its deviation from the unity, is a reactor criticality characteristic. The fundamental α-eigenvalue of the Alpha Modes spectral problem (10), under condition of its separation from other eigenvalues, is the basic characteristic of dynamic processes at relatively large times, when the regular regime takes place. Only the fundamental δ-eigenvalue of Delta Modes spectral problem (11) is connected with the whole neutron distribution behavior (see a priori estimate (13) for the solution norm) at any time moment. The difference between δ and α is a measure of not self-adjoint effect (non-symmetricity) of the problem operator, which is, in particular, due to neutron transition between separate groups. On the basis of the fundamental δ-eigenvalue of Delta Modes spectral problem we can analyze the evolution problem in details; define a stability estimate for the problem solution at differential and discrete levels.

The corresponding spectral problems for the system of Eqs. (1) and (2) are similarly formulated taking into account the delayed neutrons — total modes Verdu et al., 2010. Let's introduce the vector of density of delayed neutron sources $c = \{c_1, c_2, \ldots, c_M\}$. The Eq. (1) will be written in the form:

$$V\frac{d\phi}{dt} + (D + S)\phi = R\phi + Bc, \tag{14}$$

where now

$$R = (r_{gg'}), \quad r_{gg'} = (1 - \beta)\chi_g, \quad g, g' = 1, 2, \ldots, G,$$

and B — a rectangular matrix:

$$B = (b_{gm}), \quad b_{gm} = \widetilde{\chi}_g\lambda_m, \quad g = 1, 2, \ldots, G, \quad m = 1, 2, \ldots, M.$$

The Eq. (2) in the vector–matrix designations has the form:

$$\frac{dc}{dt} + \Lambda c = Q\phi, \tag{15}$$

at

$$\Lambda = (\lambda_{mm'}), \quad \lambda_{mm'} = \lambda_m\delta_{mm'}, \quad m, m' = 1, 2, \ldots, M,$$

$$Q = (q_{mg}), \quad q_{mg} = \beta_m\nu\Sigma_{fg}, \quad m = 1, 2, \ldots, M, \quad g = 1, 2, \ldots, G.$$

Initial conditions (4) will give

$$\phi(0) = \phi^0, \quad c(0) = c^0, \tag{16}$$

where $c^0 = \{c_1^0, c_2^0, \ldots, c_M^0\}$.

The spectral problems that are similar to (9)–(11) are used for characterization of dynamic processes, which are described by the Cauchy problem (14)–(16). The spectral problem (9) can be matched with the spectral problem

$$(D + S)\varphi = \lambda^{(k)}(R\varphi + Bs),$$
$$\Lambda s = \lambda^{(k)}Q\varphi.$$

The spectral problems, for example, of form (10) can be formulated similarly. In this case one can get

$$(D + S - R)\varphi - Bs = \lambda^{(\alpha)}V\varphi,$$
$$\Lambda s - Q\varphi = \lambda^{(\alpha)}s.$$

The analogous of the spectral problem (11) looks a little be more cumbersome, when the self-adjoint part of the problems operator is separated.

4. Numerical examples

We shall give some results of eigenvalue calculation. The elementary two-group model ($G = 2$) is used. With reference to the problem (9) one can obtain ($\Sigma_{s,2\to1} = 0$)

$$\begin{aligned} &-\nabla\cdot D_1\nabla\varphi_1 + \Sigma_{r1}\varphi_1 = \lambda^{(k)}(\nu\Sigma_{f1}\varphi_1 + \nu\Sigma_{f2}\varphi_2),\\ &-\nabla\cdot D_2\nabla\varphi_2 + \Sigma_{r2}\varphi_2 - \Sigma_{s,1\to2}\varphi_1 = 0. \end{aligned} \tag{17}$$

Now we give the spectral problem (10). Within the used two-group approximation:

$$\begin{aligned} &-\nabla\cdot D_1\nabla\varphi_1 + \Sigma_{r1}\varphi_1 - (\nu\Sigma_{f1}\varphi_1 + \nu\Sigma_{f2}\varphi_2) = \lambda^{(\alpha)}\frac{1}{v_1}\varphi_1,\\ &-\nabla\cdot D_2\nabla\varphi_2 + \Sigma_{r2}\varphi_2 - \Sigma_{s,1\to2}\varphi_1 = \lambda^{(\alpha)}\frac{1}{v_2}\varphi_2. \end{aligned} \tag{18}$$

The following problem is compared with the spectral problem (11) in two-group approximation:

$$\begin{aligned} &-\nabla\cdot D_1\nabla\varphi_1 + (\Sigma_{r1} - \nu\Sigma_{f1})\varphi_1 - \frac{1}{2}(\nu\Sigma_{f2} + \Sigma_{s,1\to2})\varphi_2 = \lambda^{(\delta)}\frac{1}{v_1}\varphi_1,\\ &-\nabla\cdot D_2\nabla\varphi_2 + \Sigma_{r2}\varphi_2 - \frac{1}{2}(\nu\Sigma_{f2} + \Sigma_{s,1\to2})\varphi_1 = \lambda^{(\delta)}\frac{1}{v_2}\varphi_2. \end{aligned} \tag{19}$$

The method of finite elements (Brenner and Scott, 2008; Quarteroni and Valli, 2008) on triangular calculation grids is used for the approximate solution of the spectral problem. The number of triangles per one assembly κ varies from 6 to 96 (Fig. 1). The standard Lagrangian finite elements of degree $p = 1, 2, 3$ are used. The software has been developed using the engineering and scientific calculation library FEniCS (Logg et al., 2012). SLEPc Hernandez et al. (2003, 2005) has been used for numerical solution of the spectral problems.

To solve spectral problems with non-symmetrical matrices we use the SLEPc (Scalable Library for Eigenvalue Problem Computations, http://slepc.upv.es/). We use a Krylov–Schur algorithm, a variation of Arnoldi method, proposed by Stewart, 2001. The error estimates used for the convergence test are based on the residual norm and the value of the tolerance is 10^{-15}.

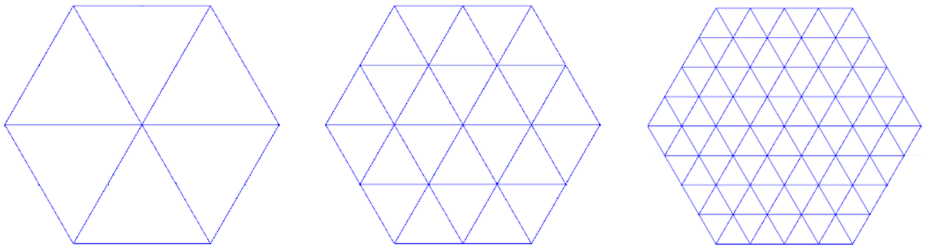

Fig. 1. Discretization of assembly into 6, 24 and 96 finite elements.

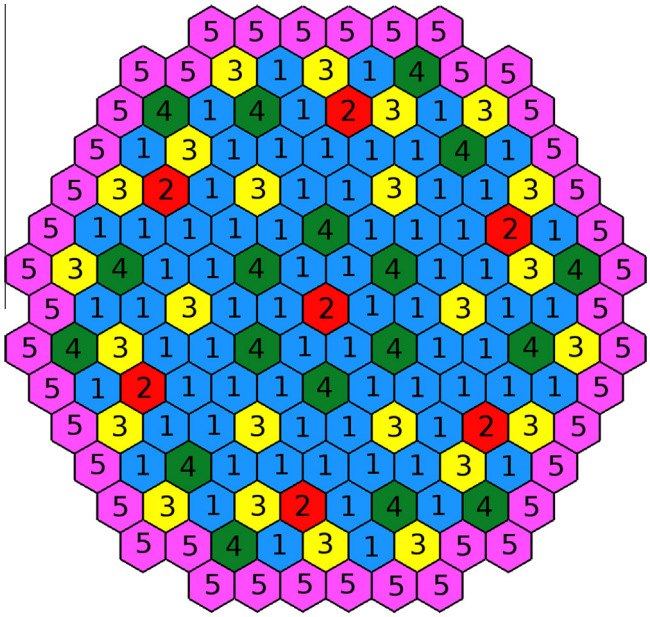

Fig. 2. Geometrcial model of the VVER-1000 reactor core.

4.1. VVER-1000 problem

The test problem for reactor VVER-1000 without reflector Chao and Shatilla, 1995 in two-dimensional approximation (Ω is the section of reactor core) is considered. The geometrical model of the VVER-1000 reactor core consists of a set of hexagonal assemblies and is presented in Fig. 2, where the assemblies of various types are marked with various digits. The total size of assembly equals 23.6 cm. Diffusion neutronics constants in the common units are given in Table 1. The boundary conditions (2) are used at $\gamma_g = 0.5,\ g = 1,2$.

4.1.1. Solution of Lambda Modes spectral problem

The results of solution of the spectral problem (17) for the first eigenvalues $k_n = 1/\lambda_n^{(k)},\ n = 1,2,\ldots,5,\ \lambda_1^{(k)} \leqslant \lambda_2^{(k)} \leqslant \ldots$ using the different grids and finite elements are shown in Table 2. These data demonstrate the convergence of approximate computed eigenvalues as the computational grid crowds and degree of the approximating polynomials increases — $h-p$ finite element method Vidal-Ferrandiz et al., 2014.

For the test under consideration, the eigenvalues $k_2, k_3, k_4, k_5, k_9, k_{10}$ of the spectral problem (9) are the complex values with small imaginary parts, and the eigenvalues k_1, k_6, k_7, k_8 are the real values. Below we give the graphs of real and imaginary parts of $\varphi^{(n)}$ eigenfunctions which correspond to the first eigenvalues $k_n,\ n = 1,2,\ldots,5$. They were calculated using a computational grid with 96 triangles for one assembly and the finite elements of the third degree. The eigenfunctions are normalized so that the norm of real or imaginary part is equal to 1, for example:

$$\|\mathrm{Re}\ \varphi_g^{(n)}\| = 1, \quad g = 1,2.$$

Table 1
Diffusion neutronics constants for VVER-100.

Material	1	2	3	4	5
D_1	1.38320e−0	1.38299e−0	1.39522e−0	1.39446e−0	1.39506e−0
D_2	3.86277e−1	3.89403e−1	3.86225e−1	3.87723e−1	3.84492e−1
Σ_{r1}	2.48836e−2	2.62865e−2	2.45662e−2	2.60117e−2	2.46141e−2
Σ_{r2}	6.73049e−2	8.10328e−2	8.44801e−1	9.89671e−2	8.93878e−2
$\Sigma_{s,1\to2}$	1.64977e−2	1.47315e−2	1.56219e−2	1.40185e−2	1.54981e−2
$\nu\Sigma_{f1}$	4.81619e−3	4.66953e−3	6.04889e−3	5.91507e−3	6.40256e−3
$\nu\Sigma_{f2}$	8.46154e−2	8.52264e−2	1.19428e−1	1.20497e−1	1.29281e−1

Table 2
The eigenvalues $k_n = 1/\lambda_n^{(k)},\ n = 1,2,\ldots,5$.

κ	p	k_1	k_2, k_3	k_4, k_5
6	1	1.00483	0.99272 ± 1.12018e−06i	0.97055 ± 1.18100e−06i
	2	1.00640	0.99473 ± 1.31480e−06i	0.97362 ± 2.49505e−06i
	3	1.00645	0.99481 ± 1.52505e−06i	0.97376 ± 2.89368e−06i
24	1	1.00600	0.99422 ± 1.55055e−06i	0.97285 ± 2.95842e−06i
	2	1.00645	0.99480 ± 1.51144e−06i	0.97376 ± 2.87450e−06i
	3	1.00634	0.99482 ± 1.51566e−06i	0.97377 ± 2.88024e−06i
96	1	1.00645	0.99466 ± 1.52518e−06i	0.97353 ± 2.90209e−06i
	2	1.00645	0.99482 ± 1.51541e−06i	0.97377 ± 2.87990e−06i
	3	1.00646	0.99482 ± 1.51558e−06i	0.97378 ± 2.88002e−06i

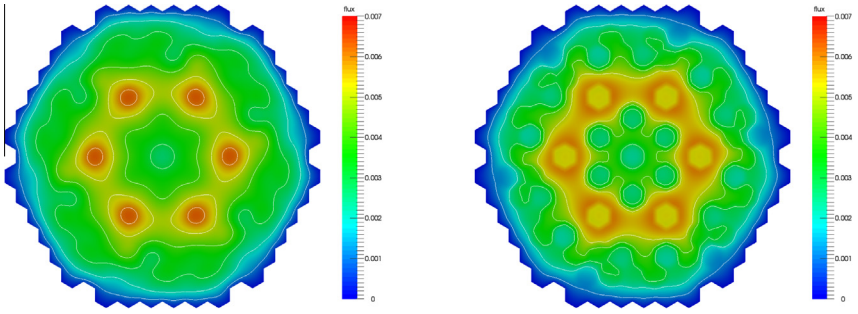

Fig. 3. The eigenfunctions $\varphi_1^{(1)}$ (left) and $\varphi_2^{(1)}$ (right).

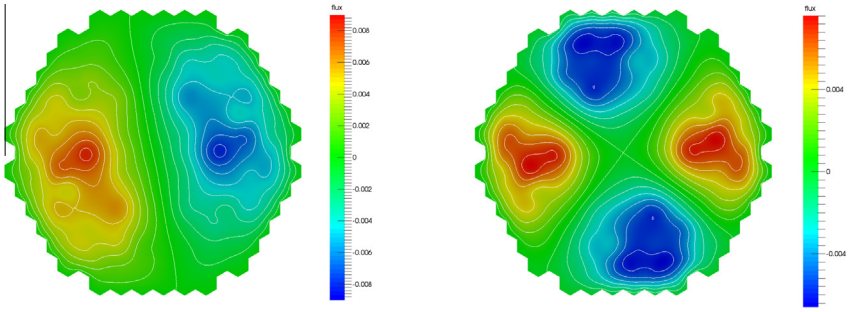

Fig. 4. Real part of eigenfunctions $\varphi_1^{(2)}$, $\varphi_1^{(3)}$ (left) and $\varphi_1^{(4)}$, $\varphi_1^{(5)}$ (right).

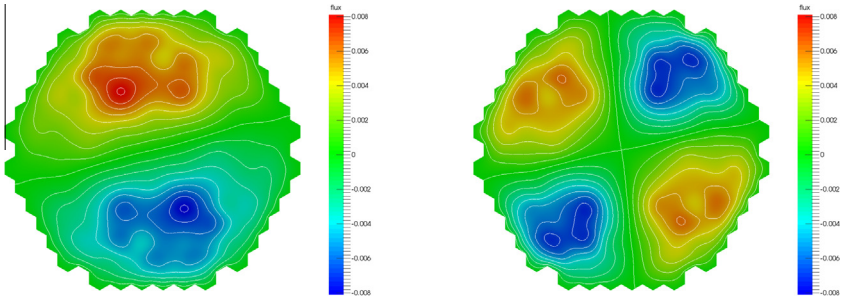

Fig. 5. Imaginary part of eigenfunctions $\varphi_1^{(2)}, -\varphi_1^{(3)}$ (left) and $\varphi_1^{(4)}, -\varphi_1^{(5)}$ (right).

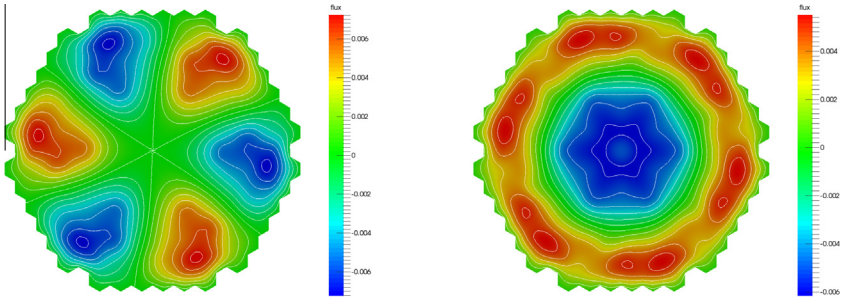

Fig. 6. The eigenfunctions $\varphi_1^{(6)}$ (left) and $\varphi_1^{(7)}$ (right).

The eigenfunctions for fundamental eigenvalue ($n = 1$) are shown in the Fig. 3. The real part of the eigenfunctions $\varphi_1^{(n)}$, $n = 2, 3, 4, 5$ is shown in the Fig. 4. Fig. 5 shows the imaginary part of the eigenfunctions. Fig. 6 shows the eigenfunctions $\varphi_1^{(6)}$ at $k_6 \approx 0.95520$ and $\varphi_1^{(7)}$ at $k_7 \approx 0.94838$.

The obtained results for the Lambda Modes spectral problem can be compared with the results obtained by González-Pintor et al. (2009). Using the high order finite element method for the test problem (VVER-1000 reactor without a reflector) they give the following eigenvalues:

$$k_1 = 1.0064540, \quad k_2 = 0.9948153, \quad k_3 = 0.9948153, \quad k_4 = 0.9737733.$$

These values are close to our calculational results for real parts of these eigenvalues. In particular, the second and third eigenval-

Table 3
The eigenvalues $\alpha_n = \lambda_n^{(\alpha)},\ n = 1, 2, \ldots, 5$.

κ	p	α_1	α_2, α_3	α_4, α_5
6	1	−105.032	159.802 ± 0.025510i	659.109 ± 0.034667i
	2	−139.090	115.793 ± 0.029186i	591.782 ± 0.034667i
	3	−140.223	114.035 ± 0.033814i	588.762 ± 0.069025i
24	1	−130.422	126.984 ± 0.034409i	608.734 ± 0.070724i
	2	−140.187	114.089 ± 0.033512i	588.849 ± 0.068555i
	3	−140.281	113.887 ± 0.033604i	588.415 ± 0.068695i
96	1	−137.704	117.345 ± 0.033823i	593.818 ± 0.069254i
	2	−140.284	113.886 ± 0.033599i	588.419 ± 0.068687i
	3	−140.308	113.842 ± 0.033603i	588.336 ± 0.068690i

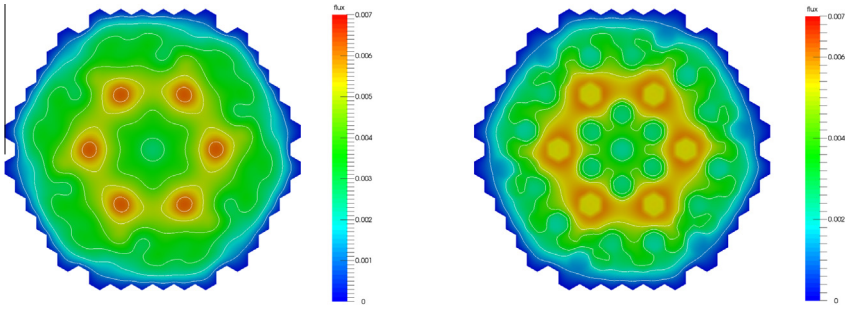

Fig. 7. The eigenfunctions $\varphi_1^{(1)}$ (left) and $\varphi_2^{(1)}$ (right).

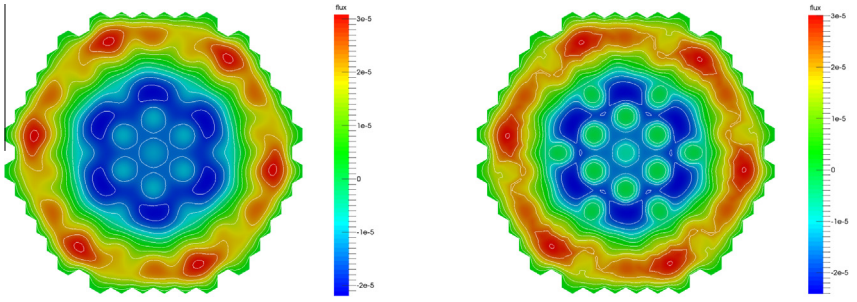

Fig. 8. Difference of eigenfunctions $\delta\varphi_1^{(1)}$ (left) and $\delta\varphi_2^{(1)}$ (right).

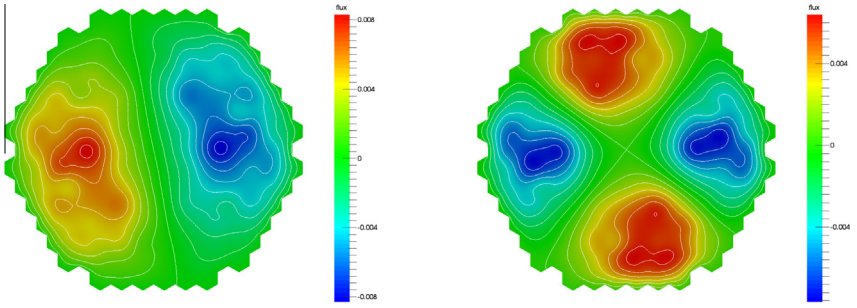

Fig. 9. Real part of eigenfunctions $\varphi_1^{(2)},\ \varphi_1^{(3)}$ (left) and $\varphi_1^{(4)},\ \varphi_1^{(5)}$ (right).

ues are equal. The principal point is the complexity of the eigenvalues with small imaginary parts and we proved this fact.

4.1.2. Solution of Alpha Modes spectral problem

The problem (18) is solved at $\nu_1 = 12,500,000$ and $\nu_2 = 250,000$. The results of solution of the spectral problem (18) for the first eigenvalues $\alpha_n = \lambda_n^{(\alpha)},\ n = 1, 2, \ldots, 5,\ \lambda_1^{(\alpha)} \leqslant \lambda_2^{(\alpha)} \leqslant \ldots$ at different computational grids using different finite-element approximations are shown in Table 3. The eigenvalues $\alpha_2, \alpha_3, \alpha_4, \alpha_5, \alpha_9, \alpha_{10}$ of the spectral problem (10), like for the spectral problem (9), are the complex values with small imaginary parts, and the eigenvalues $\alpha_1, \alpha_6, \alpha_7, \alpha_8$ are the real values.

The eigenfunctions for fundamental eigenvalue ($n = 1$) of the spectral problem (18) are shown in the Fig. 7. Due to the fact that a state of the reactor is close to critical ($k = k_1 \approx 1.00646$), the fundamental eigenfunctions of the spectral problem (17) are close to the fundamental eigenfunctions of the spectral problem (18). Fig. 8 shows the difference of α-eigenfunction and λ-eigenfunction.

The real part of the eigenfunctions $\varphi_1^{(n)},\ n = 2, 3, 4, 5$ is shown in the Fig. 9. Fig. 10 shows the imaginary part of these eigenfunc-

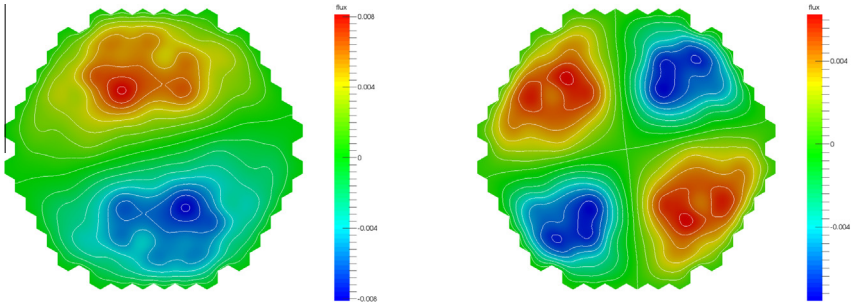

Fig. 10. Imaginary part of eigenfunctions $\varphi_1^{(2)}, -\varphi_1^{(3)}$ (left) and $\varphi_1^{(4)}, -\varphi_1^{(5)}$ (right).

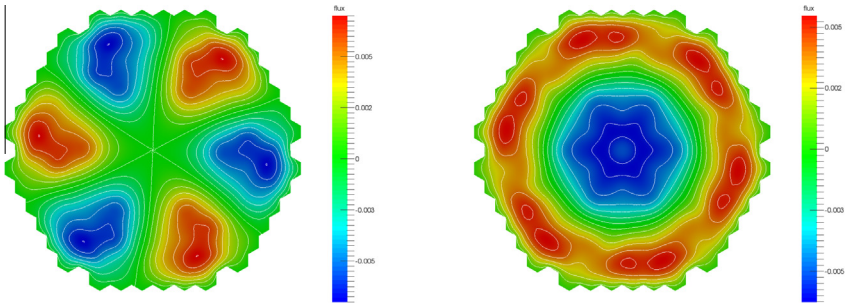

Fig. 11. The eigenfunctions $\varphi_1^{(6)}$ (left) and $\varphi_1^{(7)}$ (right).

Table 4
The eigenfunctions $\delta_n = \lambda_n^{(\delta)}$, $n = 1, 2, \ldots, 5$.

κ	p	δ_1	δ_2	δ_3	δ_4	δ_5
	1	−22170.12	−22058.40	−22058.39	−21768.84	−21768.82
6	2	−22933.98	−22830.17	−22830.16	−22563.69	−22563.67
	3	−22982.60	−22878.57	−22878.56	−22611.14	−22611.12
	1	−22745.06	−22639.74	−22639.73	−22369.01	−22368.99
24	2	−22923.50	−22819.17	−22819.17	−22551.00	−22550.98
	3	−22989.87	−22885.85	−22885.84	−22618.47	−22618.44
	1	−22923.50	−22819.17	−22819.17	−22551.00	−22550.98
96	2	−22989.61	−22885.60	−22885.59	−22618.22	−22618.20
	3	−22991.05	−22887.04	−22887.03	−22619.66	−22619.63

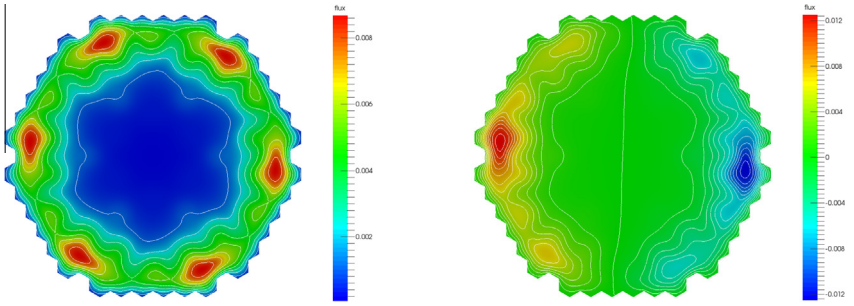

Fig. 12. The eigenfunctions $\varphi_1^{(1)}$ (left) and $\varphi_1^{(2)}$ (right).

tions. Fig. 11 shows the eigenfunctions $\varphi_1^{(6)}$ at $\alpha_6 \approx 1028.440$ and $\varphi_1^{(7)}$ at $\alpha_7 \approx 1180.547$.

The first eigenfunctions of the problems (17) and (18) are close to each other in topology. The eigenvalues $\lambda_1^{(\alpha)} \leqslant \lambda_2^{(\alpha)} \leqslant \ldots$ are well separated. In our example, the fundamental eigenvalue is negative and therefore the main harmonic will increase, while all others will attenuate. A regular mode of the reactor is thereby defined. The value $\alpha = \lambda_1^{(\alpha)}$ determines the amplitude of neutron field development and connects directly with reactor period in the regular mode.

4.1.3. Solution of Delta Modes spectral problem

The results of solution of this spectral problem for the first five eigenvalues are shown in Table 4. All the eigenvalues are real, and

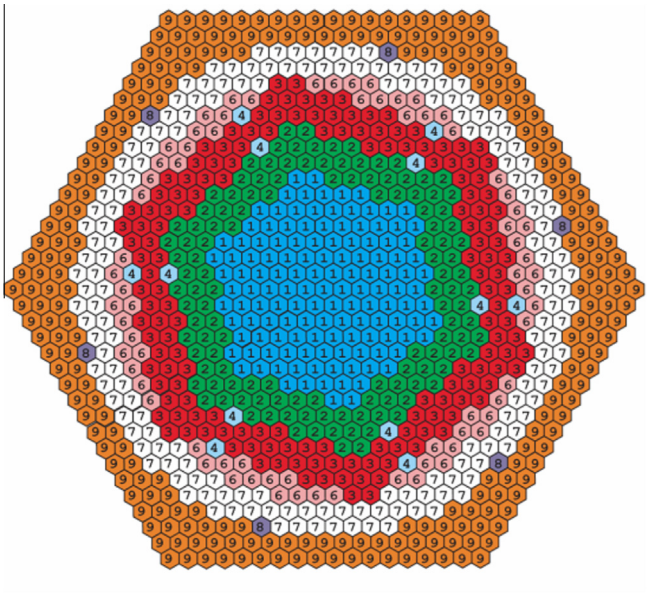

Fig. 13. Geometrcial model of the HWR reactor core.

the value $\delta = \delta_1 \approx -22991.05$ is far enough from the value $\alpha = \alpha_1 \approx -140.308$. The eigenvalues of the problem (19) are of little importance. Therefore only $\varphi_1^{(1)}$ and $\varphi_1^{(2)}$ are given in Fig. 12.

4.2. HWR problem

This benchmark simulate the active zone of a large heavy-water reactor HWR Chao and Shatilla, 1995. The geometrical model of the HWR reactor core consists of a set of hexagonal assemblies and is presented in Fig. 13. The total size of assembly equals 17.78 cm. Diffusion neutronics constants in the common units are given in Table 5. The boundary conditions (2) are used at $\gamma_g = 0.5, g = 1, 2$.

4.2.1. Solution of Lambda Modes spectral problem

The results of solution of the spectral problem (17) for the first eigenvalues $k_n = 1/\lambda_n^{(k)},\ n = 1, 2, \ldots, 5,\ \lambda_1^{(k)} \leqslant \lambda_2^{(k)} \leqslant \ldots$ using the different grids and finite elements are shown in Table 6. We have the convergence of approximate computed eigenvalues as the computational grid crowds and degree of the approximating polynomials increases.

The eigenvalues $k_2, k_3, k_4, k_5, k_9, k_{10}$ of the spectral problem (9) are the complex values with small imaginary parts, and the eigenvalues k_1, k_6, k_7, k_8 are the real values. We give the graphs of real and imaginary parts of $\varphi^{(n)}$ eigenfunctions which correspond to the first eigenvalues $k_n,\ n = 1, 2, \ldots, 5$. The eigenfunctions for fundamental eigenvalue ($n = 1$) are shown in the Fig. 14. The real part of the eigenfunctions $\varphi_1^{(n)},\ n = 2, 3, 4, 5$ is shown in the Fig. 15. Fig. 16 shows the imaginary part of the eigenfunctions.

For this test problem (HWR reactor) González-Pintor et al. (2009) give the following eigenvalues:

$$k_1 = 0.9919610, \quad k_2 = 0.9835926, \quad k_3 = 0.9835926,$$
$$k_4 = 0.9642380.$$

These values are close to our results for real parts of these eigenvalues.

4.2.2. Solution of Alpha Modes spectral problem

The problem (18) is solved at $\nu_1 = 12,500,000$ and $\nu_2 = 250,000$. The results of solution of the spectral problem

Table 5
Diffusion neutronics constants for HWR.

Material	Group	D	Σ_r	$\Sigma_{1\to 2}$	$\nu\Sigma_f$
1	1	1.38250058	1.1105805e−2	8.16457e−3	2.26216e−3
	2	0.89752185	2.2306487e−2		2.30623e−2
2	1	1.38255219	1.1174585e−2	8.22378e−3	2.22750e−3
	2	0.89749043	2.2387609e−2		2.26849e−2
3	1	1.37441741	1.0620368e−2	8.08816e−3	2.14281e−3
	2	0.88836771	1.6946527e−2		2.04887e−2
4	1	1.31197955	1.2687953e−2	1.23115e−2	0.0
	2	0.87991376	5.2900925e−2		0.0
6	1	1.38138909	1.056312e−2	7.76568e−3	2.39469e−3
	2	0.90367052	2.190298e−2		2.66211e−2
7	1	1.30599110	1.1731321e−2	1.10975e−2	0.0
	2	0.83725587	4.3330365e−3		0.0
8	1	1.29192957	1.1915316e−2	1.15582e−2	0.0
	2	0.81934103	3.0056488e−4		0.0
9	1	1.06509884	2.8346221e−2	2.61980e−2	0.0
	2	0.32282849	3.3348874e−2		0.0

Table 6
The eigenvalues $k_n = 1/\lambda_n^{(k)},\ n = 1, 2, \ldots, 5$.

κ	p	k_1	k_2, k_3	k_4, k_5
	1	0.99198	0.98360 ± 1.06467e−05i	0.96414 ± 1.96893e−05i
6	2	0.99199	0.98362 ± 1.16182e−05i	0.96427 ± 2.15201e−05i
	3	0.99196	0.98360 ± 1.16441e−05i	0.96424 ± 2.15627e−05i
	1	0.99198	0.98361 ± 1.13901e−05i	0.96423 ± 2.10911e−05i
24	2	0.99197	0.98360 ± 1.16422e−05i	0.96424 ± 2.15595e−05i
	3	0.99196	0.99359 ± 1.16449e−05i	0.96424 ± 2.15643e−05i
	1	0.99197	0.98360 ± 1.15799e−05i	0.96424 ± 2.14440e−05i
96	2	0.99196	0.98359 ± 1.16448e−05i	0.96424 ± 2.15640e−05i
	3	0.99196	0.98359 ± 1.16447e−05i	0.96424 ± 2.15639e−05i

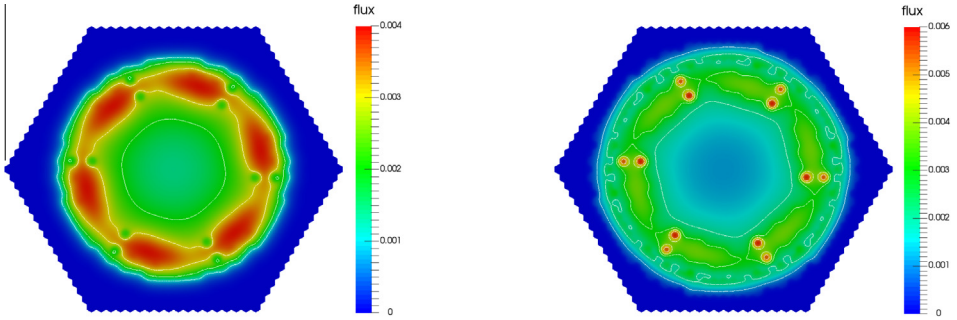

Fig. 14. The eigenfunctions $\varphi_1^{(1)}$ (left) and $\varphi_2^{(1)}$ (right).

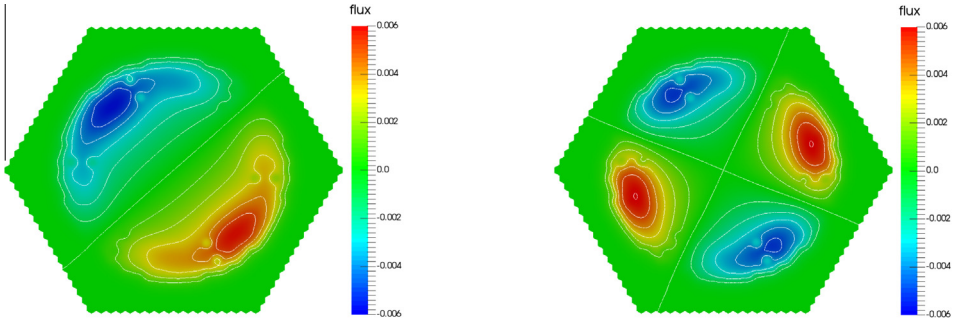

Fig. 15. Real part of eigenfunctions $\varphi_1^{(2)}$, $\varphi_1^{(3)}$ (left) and $\varphi_1^{(4)}$, $\varphi_1^{(5)}$ (right).

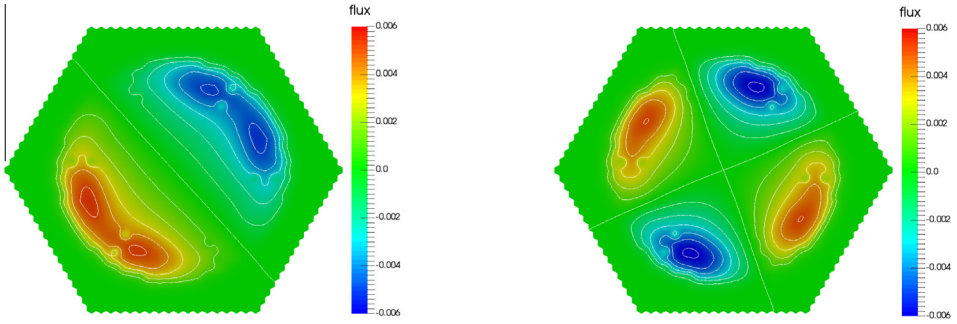

Fig. 16. Imaginary part of eigenfunctions $\varphi_1^{(2)}, -\varphi_1^{(3)}$ (left) and $\varphi_1^{(4)}, -\varphi_1^{(5)}$ (right).

Table 7
The eigenvalues $\alpha_n = \lambda_n^{(\alpha)}$, $n = 1, 2, \ldots, 5$.

κ	p	α_1	α_2, α_3	α_4, α_5
6	1	42.28145	85.12917 ± 0.05604i	183.97351 ± 0.10320i
	2	42.13522	84.73725 ± 0.06117i	182.79517 ± 0.11345i
	3	42.25852	84.86342 ± 0.06130i	182.91188 ± 0.11367i
24	1	42.19593	84.86062 ± 0.05997i	183.11506 ± 0.11104i
	2	42.25260	84.85735 ± 0.06129i	182.90628 ± 0.11365i
	3	42.26300	84.86756 ± 0.06130i	182.91450 ± 0.11367i
96	1	42.24114	84.86101 ± 0.06096i	182.96129 ± 0.11301i
	2	42.26235	84.86689 ± 0.06130i	182.91391 ± 0.11367i
	3	42.26266	84.86709 ± 0.06130i	182.91375 ± 0.11367i

(18) for the first eigenvalues $\alpha_n = \lambda_n^{(\alpha)}$, $n = 1, 2, \ldots, 5$, $\lambda_1^{(\alpha)} \leqslant \lambda_2^{(\alpha)} \leqslant \ldots$ at different computational grids using different finite-element approximations are shown in Table 7. The eigenvalues $\alpha_2, \alpha_3, \alpha_4, \alpha_5, \alpha_9, \alpha_{10}$ of the spectral problem (10), like for the spectral problem (9), are the complex values with small imaginary parts, and the eigenvalues $\alpha_1, \alpha_6, \alpha_7, \alpha_8$ are the real values.

The eigenfunctions for fundamental eigenvalue ($n = 1$) of the spectral problem (18) are shown in the Fig. 17. The real part of the eigenfunctions $\varphi_1^{(n)}$, $n = 2, 3, 4, 5$ is shown in the Fig. 18. Fig. 19 shows the imaginary part of these eigenfunctions. The first eigenfunctions of the problems (17) and (18) are close to each other in topology. The eigenvalues $\lambda_1^{(\alpha)} \leqslant \lambda_2^{(\alpha)} \leqslant \ldots$ are well separated.

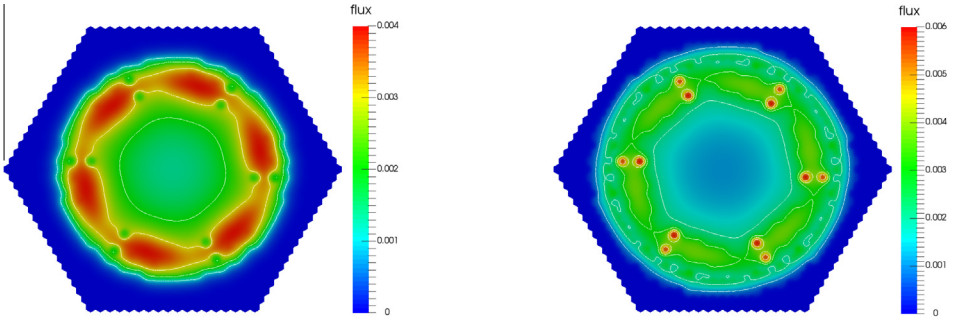

Fig. 17. The eigenfunctions $\varphi_1^{(1)}$ (left) and $\varphi_2^{(1)}$ (right).

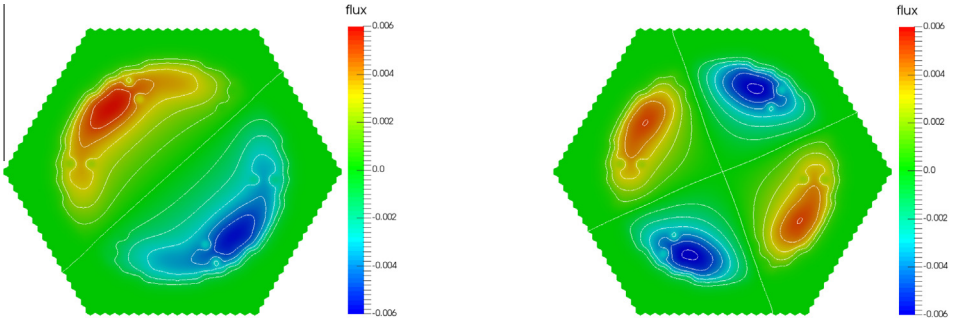

Fig. 18. Real part of eigenfunctions $\varphi_1^{(2)}, \varphi_1^{(3)}$ (left) and $\varphi_1^{(4)}, \varphi_1^{(5)}$ (right).

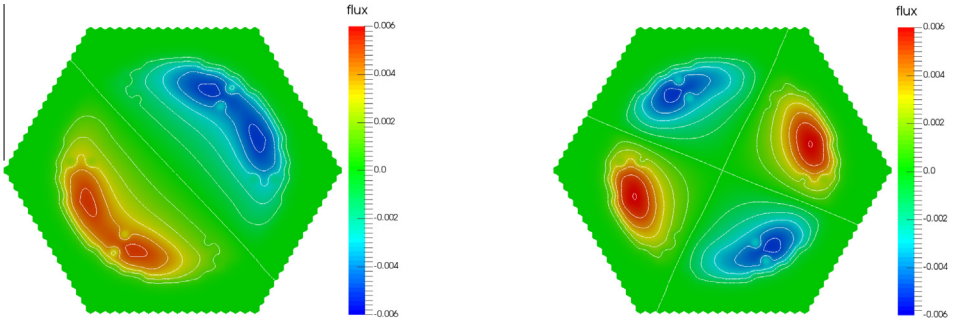

Fig. 19. Imaginary part of eigenfunctions $\varphi_1^{(2)}, -\varphi_1^{(3)}$ (left) and $\varphi_1^{(4)}, -\varphi_1^{(5)}$ (right).

Table 8
The eigenfunctions $\delta_n = \lambda_n^{(\delta)}$, $n = 1, 2, \ldots, 5$.

κ	p	δ_1	δ_2	δ_3	δ_4	δ_5
6	1	−1127.55257	−1009.80617	−1009.80398	−871.60140	−871.59855
	2	−1132.64216	−1018.75605	−1018.75385	−883.21855	−883.21571
	3	−1132.81177	−1019.03389	−1019.03169	−883.53871	−883.53587
24	1	−1131.36452	−1016.52656	−1016.52435	−880.32945	−880.32661
	2	−1132.80333	−1019.02010	−1019.01790	−883.52291	−883.52007
	3	−1132.82161	−1019.05019	−1019.04798	−883.55788	−883.55504
96	1	−1132.44380	−1018.39826	−1018.39605	−882.72667	−882.72383
	2	−1132.82067	−1019.04865	−1019.04644	−883.55611	−883.55327
	3	−1132.82240	−1019.05153	−1019.04932	−883.55955	−883.55671

4.2.3. Solution of Delta Modes spectral problem

The results of solution of this spectral problem for the first five eigenvalues are shown in Table 8. All the eigenvalues are real, and the value $\delta = \delta_1 \approx -1132.82$ is far enough from the value $\alpha = \alpha_1 \approx 42.26$. Eigenfunctions $\varphi_1^{(1)}$ and $\varphi_1^{(2)}$ are given in Fig. 20.

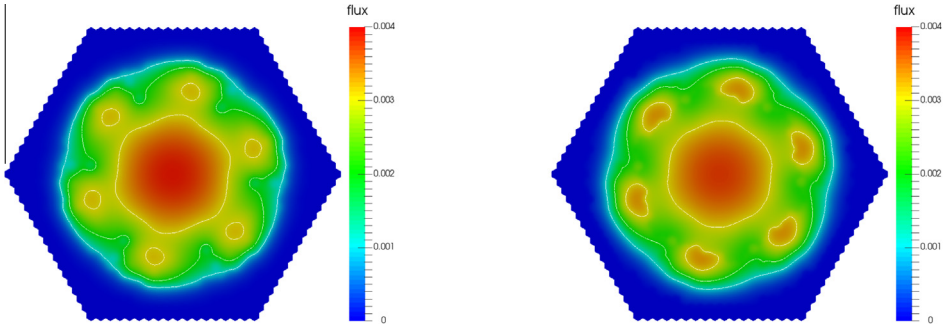

Fig. 20. The eigenfunctions $\varphi_1^{(1)}$ (left) and $\varphi_1^{(2)}$ (right).

5. Conclusions

The spectral problems that may characterize the reactor dynamic behavior are considered. Within the multi-group diffusion approximation, the standard Lambda Modes spectral problem which is related to the definition of k-effective of the reactor core is considered. The Alpha Modes spectral problem is much more informative for considering the dynamic processes. We can relate the dynamics of the reactor at asymptotic stage at large times to fundamental α-eigenvalue and α-eigenfunction. A new spectral problem (Delta Modes spectral problem) is formulated, which is connected to self-adjoint part of operator of neutron absorption-generation. Solution of this problem allows making an a priori estimate of neutron flux dynamics.

The computational algorithm for approximate solution of the spectral problems is based on a standard finite-element approximation using Lagrange finite elements of $p = 1, 2, 3$. The matrix spectral problem is solved using a scalable and flexible toolkit for the solution of eigenvalue problems SLEPc. Approximate solution accuracy is checked at a sequence of condensing grid using finite elements of varying degrees.

Test calculations are made in two-dimensional approximation for a model of VVER-1000 reactor without reflector and and HWR reactor using two-group diffusion approximation. The first real and complex eigenvalues and eigenfunctions in the Lambda Modes spectral problem are got. A good separability of the eigenvalues in the Alpha Modes spectral problem is identified. The results of the numerical solution of the Delta Modes spectral problem to assess neutron flux dynamics are given.

Acknowledgements

This work was supported by the Russian Foundation for Basic Research (project 16-08-01215).

References

Ascher, U.M., 2008. Numerical Methods for Evolutionary Differential Equations. Society for Industrial Mathematics.
Bell, G.I., Glasstone, S., 1970. Nuclear Reactor Theory. Van Nostrand Reinhold Company.
Boyd, W., Shaner, S., Li, L., Forget, B., Smith, K., 2014. The openMOC method of characteristics neutral particle transport code. Ann. Nucl. Energy 68, 43–52.
Brenner, S.C., Scott, R., 2008. The Mathematical Theory of Finite Element Methods. Springer.
Butcher, J.C., 2008. Numerical Methods for Ordinary Differential Equations. Wiley.
Chao, Y.A., Shatilla, Y.A., 1995. Conformal mapping and hexagonal nodal methods-II: implementation in the ANC-H Code. Nucl. Sci. Eng. 121, 210–225.
Cho, N.Z., 2005. Fundamentals and recent developments of reactor physicsmethods. Nucl. Eng. Technol. 37 (1), 25–78.
Chou, H.P., Lu, J.R., Chang, M.B., 1990. A three-dimensional space-time model and its use in pressurized water reactor rod ejection analyses. Nucl. Technol. 90 (2), 142–154.
Dahmani, M., Baudron, A.M., Lautard, J.J., Erradi, L., 2001. A 3D nodal mixed dual method for nuclear reactor kinetics with improved quasistatic model and a semi-implicit scheme to solve the precursor equations. Ann. Nucl. Energy 28 (8), 805–824.
Dodds Jr, H.L., 1976. Accuracy of the quasistatic method for two-dimensional thermal reactor transients with feedback. Nucl. Sci. Eng. 59 (3), 271–276.
Duderstadt, J.J., Hamilton, L.J., 1976. Nuclear Reactor Analysis. Wiley.
Dugan, K., Zmijarevic, I., Sanchez, R., 2016. Cross-section homogenization for reactivity-induced transient calculations. J. Comput. Theor. Transp., 1–17 (Published online: 15 Jul 2016)
Evans, L.C., 1998. Partial Differential Equations. American Mathematical Society.
Golub, G.H., Van Loan, C.F., 2012. Matrix Computations. Johns Hopkins University Press.
Goluoglu, S., Dodds, H.L., 2001. A time-dependent, three-dimensional neutron transport methodology. Nucl. Sci. Eng. 139 (3), 248–261.
González-Pintor, S., Ginestar, D., Verdú, G., 2009. High order finite element method for the lambda modes problem on hexagonal geometry. Ann. Nucl. Energy 36 (9), 1450–1462.
Habetler, G.J., Martino, M.A., 1961. Existence theorems and spectral theory for the multigroup diffusion model. Nucl. Reactor Theory Proc. Symp. Appl. Math., vol. 11, pp. 127–139.
Hairer, E., Wanner, G., 2010. Solving Ordinary Differential Equations II: Stiff and Differential-Algebraic Problems. Springer Verlag.
Hernandez, V., Roman, J.E., Vidal, V., 2005. SLEPc: a scalable and flexible toolkit for the solution of eigenvalue problems. ACM Trans. Math. Software (TOMS) 31 (3), 351–362.
Hernandez, V., Roman, J.E., Vidal, V., Verdu, G., Ginestar, D., 2003. Resolution of the neutron diffusion equation with SLEPc, the scalable library for eigenvalue problem computations. Nuclear Mathematical and Computational Sciences: A Century in Review, A Century Anew Gatlinburg. American Nuclear Society, pp. 1–10.
Hetrick, D.L., 1971. Dynamics of Nuclear Reactors. University of Chicago Press.
Hogben, L. (Ed.), 2013. Handbook of Linear Algebra. second ed. CRC.
Hundsdorfer, W.H., Verwer, J.G., 2003. Numerical Solution of Time-Dependent Advection-Diffusion-Reaction Equations. Springer Verlag.
LeVeque, R.J., 2007. Finite Difference Methods for Ordinary and Partial Differential Equations. Steady-State and Time-Dependent Problems. Society for Industrial Mathematics.
Lewis, E.E., Miller, W.F., 1993. Computational Methods of Neutron Transport. American Nuclear Society.
Logg, A., Mardal, K.A., Wells, G., 2012. Automated Solution of Differential Equations by the Finite Element Method: The FEniCS Book. Springer.
Luikov, A., 1968. Analytical Heat Diffusion Theory. Academic Press.
Marchuk, G.I., Lebedev, V.I., 1986. Numerical Methods in the Theory of Neutron Transport. Harwood Academic Pub.
Modak, R.S., Gupta, A., 2007. A scheme for the evaluation of dominant time-eigenvalues of a nuclear reactor. Ann. Nucl. Energy 34 (3), 213–221.
Quarteroni, A., Valli, A., 2008. Numerical Approximation of Partial Differential Equations. Springer.
Saad, Y., 2011. Numerical Methods for Large Eigenvalue Problems. SIAM.
Samarskii, A.A., 2001. The Theory of Difference Schemes. Marcel Dekker, New York.
Samarskii, A.A., Matus, P.P., Vabishchevich, P.N., 2002. Difference Schemes with Operator Factors. Kluwer.
Samarskii, A.A., Vabishchevich, P.N., 1996. Computational Heat Transfer. Wiley.
Sanchez, R., 2009. Assembly homogenization techniques for core calculations. Prog. Nucl. Energy 51 (1), 14–31.
Sanchez, R., 2012. Prospects in deterministic three-dimensional whole-core transport calculations. Nucl. Eng. Technol. 44 (2), 113–150.
Smith, K.S., Rhodes III, J.D., 2002. Full-core, 2-d, lwr core calculations with casmo-4e. In: Proc. PHYSOR, Seoul, Korea, October 7–10. pp. 1–13.
Stacey, W.M., 2007. Nuclear Reactor Physics. Wiley.
Stewart, G.W., 2001. A Krylov–Schur algorithm for large eigenproblems. SIAM J. Matrix Anal. Appl. 23 (3), 601–614.
Sutton, T.M., Aviles, B.N., 1996. Diffusion theory methods for spatial kinetics calculations. Prog. Nucl. Energy 30 (2), 119–182.
Verdu, G., Ginestar, D., Roman, J., Vidal, V., 2010. 3D alpha modes of a nuclear power reactor. J. Nucl. Sci. Technol. 47 (5), 501–514.
Vidal-Ferrandiz, A., Fayez, R., Ginestar, D., Verdú, G., 2014. Solution of the lambda modes problem of a nuclear power reactor using an $h--p$ finite element method. Ann. Nucl. Energy 72, 338–349.